Ultrafast interlayer photocarrier transfer in graphene–$MoSe_2$ van der Waals heterostructure*

Xin-Wu Zhang(张心悟), Da-Wei He(何大伟), Jia-Qi He(何佳琪), Si-Qi Zhao(赵思淇), Sheng-Cai Hao(郝生财), Yong-Sheng Wang(王永生), and Li-Xin Yi(衣立新)†

Key Laboratory of Luminescence and Optical Information, Ministry of Education, Institute of Optoelectronic Technology, Beijing Jiaotong University, Beijing 100044, *China*

(Received 28 April 2017; revised manuscript received 11 June 2017; published online 31 July 2017)

We report the fabrication and photocarrier dynamics in graphene–$MoSe_2$ heterostructures. The samples were fabricated by mechanical exfoliation and manual stacking techniques. Ultrafast laser measurements were performed on the heterostructure and $MoSe_2$ monolayer samples. By comparing the results, we conclude that photocarriers injected in $MoSe_2$ of the heterostructure transfer to graphene on an ultrafast time scale. The carriers in graphene alter the optical absorption coefficient of $MoSe_2$. These results illustrate the potential applications of this material in optoelectronic devices.

Keywords: van der Waals heterostructure, transition metal dichalcogenides, molybdenum diselenide, transient absorption

PACS: 72.80.Ga, 73.50.−h, 78.47.jb, 78.47.jg **DOI:** 10.1088/1674-1056/26/9/097202

1. Introduction

The discovery of graphene in 2004[1,2] has stimulated extensive studies on its novel property and potential applications. Graphene is formed by a single layer of carbon atoms bound together in a hexagonal lattice. Due to its unique structure, graphene has many superior properties, such as high Young's modulus and fracture strength,[3] high thermal conductivity,[4] ultrafast dynamic optical properties,[5] and high charge carrier mobility.[1] These properties make graphene an attractive candidate for various applications, such as ultracapacitors,[6,7] solar cells,[8–11] photodetector,[12] and low-power-consumption electronics.[13,14] However, the lack of a bandgap limited its application in logic electronic devices. Furthermore, its relatively small optical absorbance is also a drawback for optoelectronic applications. Monolayer transition metal dichalcogenides (TMDs), on the other hand, have remarkably high absorbance in the visible range[15] and a sizable bandgap.[16,17] However, their charge carrier mobilities are relatively low. Hence, combining graphene and TMD can potentially produce bi-layer materials that can effectively absorb light and transfer charge carriers, which are two key elements for most optoelectronic applications.

Indeed, very recently, significant progress has been made in studies of graphene–TMD heterostructures. So far, most studies have focused on combining graphene with MoS_2. Initially, such heterostructures were fabricated by manually stacking graphene and MoS_2 monolayers together.[18] Mechanical properties of graphene–MoS_2 were studied both theoretically and experimentally.[19,20] The electronic structure of the formed heterostructure was calculated, measured, and controlled.[21–26] For electronic applications, tunneling transistors have been demonstrated with MoS_2 serving as the tunneling barrier.[18,27–33]

Besides these investigations on graphene–MoS_2, heterostructure formed by graphene and tungsten based TMD monolayers has also been studied. For graphene–WS_2, spin–orbit interaction[34] and various applications have been attempted, such as tunneling transistors,[29,35] photovoltaics,[36] light-emitting diodes,[37] and photodetection.[38] Measurements of its band alignment,[39] photoluminescence properties,[40] and light-emitting devices[37] have been reported.

In contrast to these extensive efforts on developing heterostructures formed by graphene and MoS_2 and WS_2, $MoSe_2$ has been seldom used to form heterostructures with graphene. The only reports on graphene–$MoSe_2$ heterostructures are their molecular beam expitaxy[41] and observation of photoluminescence quenching.[42] $MoSe_2$ possesses several properties that make it an attractive member of TMDs. It has a direct optical bandgap of 1.55 eV,[43] which is near the optimal bandgap of single-junction photovoltaic devices and photocatalysis.[44–46]

Here we report fabrication of graphene–$MoSe_2$ heterostructures and ultrafast laser measurements on photocarrier dynamics. We observed efficient carrier transfer from $MoSe_2$ to graphene, and strong effect of carriers in graphene on optical properties of $MoSe_2$. These results indicate that graphene–

*Project supported by the National Natural Science Foundation of China (Grant Nos. 61275058, 61527817, 61335006, and 61378073), the National Science Foundation, China (Grant No. DMR-1505852), the National Basic Research Program of China (Grant Nos. 2016YFA0202300 and 2016YFA0202302), and Beijing Science and Technology Committee, China (Grant No. Z151100003315006).

†Corresponding author. E-mail: lxyi@bjtu.edu.cn

© 2017 Chinese Physical Society and IOP Publishing Ltd

$MoSe_2$ heterostructures are promising materials for optoelectronic applications.

2. Experiment

Graphene and $MoSe_2$ flakes were fabricated by mechanical exfoliation. Adhesive tapes were used to mechanically exfoliate flakes from bulk crystals onto polydimethylsiloxane (PDMS) substrates. The monolayers were identified by optical contrasts with an optical microscope. Then a $MoSe_2$ monolayer flake was transferred to a Si substrate with a 90 nm SiO_2 layer and annealed for 2 h at 200 °C in an Ar (60 sccm) environment with a pressure of 3 Torr. Next, a graphene flake was transferred onto the $MoSe_2$ flake, followed by the same annealing procedure. The final optical microscope image of the sample is shown in Fig. 1(a), where the graphene–$MoSe_2$ heterostructure is in the triangle yellow area. Figure 1(b) illustrates the predicted band alignment[47,48] of the heterostructure. We note that the band gap of $MoSe_2$ presented in Fig. 1(b) is a theoretical value, which is different from that of the experiment and has no influence on the measurement.

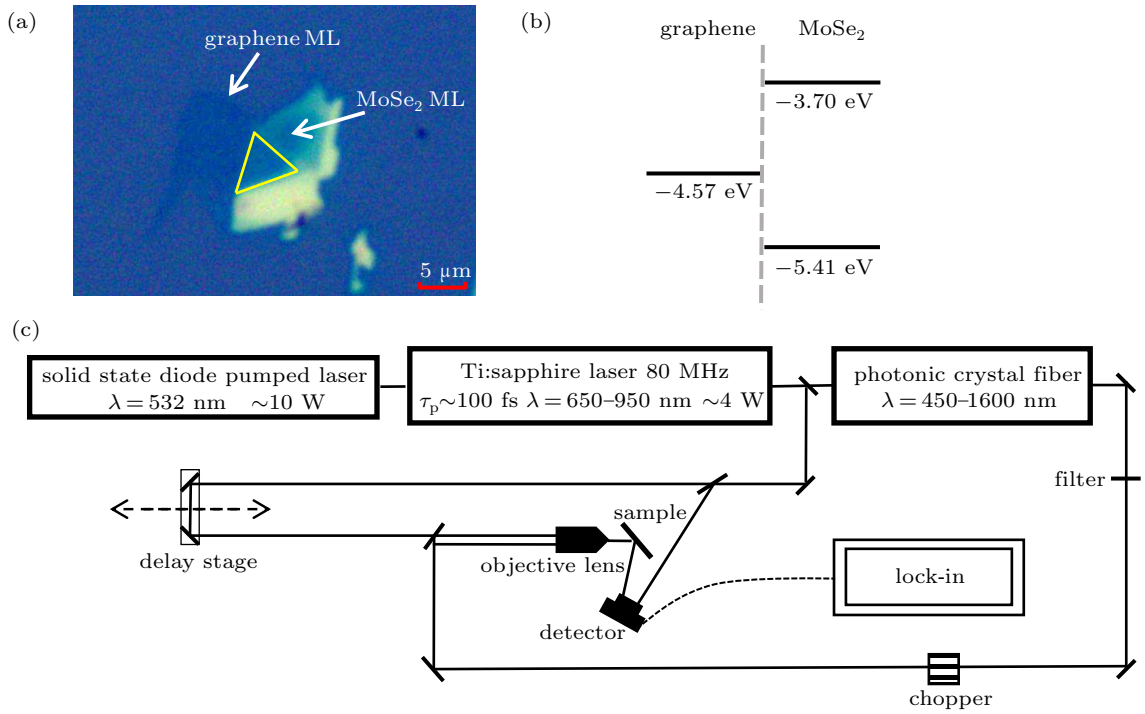


Fig. 1. (color online) (a) Microscope images of the samples studied. (b) Band alignment of graphene and $MoSe_2$ monolayers. (c) Experimental setup to measure differential reflectivity.

In the transient absorption microscopy setup shown as Fig. 1(c), a passively mode-locked Ti:sapphire oscillator was used to generate a 100 fs pulse with a central wavelength of 790 nm at 80 MHz. We used a beamsplitter to separate the pulse into two beams. One of the beams was coupled to a photonic crystal fiber to generate supercontinuum. A bandpass filter with a passing wavelength of 620 nm and a bandwidth of 10 nm was employed to select a 620 nm pulse from the supercontinuum,which served as the pump. Combined with the other beam probe which was outputted directly from the oscillator, the two beams were finally focused onto the sample by a microscope objective lens. The reflected probe was collimated by the objective lens and measured by one detector of a balanced detector. A portion of the probe beam was taken as a reference beam, which is sent to the other detector of the balanced detector. A lock-in amplifier was used to measure the voltage output of the detector. A mechanical chopper was placed in the pump arm to modulate the intensity of the pump beam at about 2 kHz. Hence, the balanced detector now outputs a voltage that is proportional to a differential reflectivity of the probe, R/R_0. It is defined as the relative change of the probe reflectivity caused by the pump, $(R\text{-}R_0)/R_0$, where R and R_0 are the reflectivity of the probe with the pump presence and without it, respectively. All the measurements were performed at room temperature with the sample exposed in air.

3. Results and discussion

We first studied a $MoSe_2$ monolayer sample. A pump pulse of 2.00 eV was used to inject photocarriers. A probe pulse of 1.57 eV, which is tuned near to the exciton resonance of $MoSe_2$, was used to monitor these photocarriers. The top panel of Fig. 2(a) shows the differential reflectivity signal as a function of the probe delay. In this measurement, the pump fluence is 4.9 μJ/cm^2. By using an absorption coeffi-

cient of 2×10^5 cm^{-1} for $MoSe_2$ monolayer at the probe photon energy,[49] an injected carrier density of 2.1×10^{10} cm^{-2} was established. A peak differential reflectivity signal of 1.14×10^{-4} was observed. Furthermore, the decay of the signal can be fitted by a bi-exponential function, with two time constants of 22 and 125 ps, respectively. The rest of Fig. 2(a) shows the measured signal at different pump fluences. By fitting these data, we found that as the pump fluence decreased, the fast decay component characterized by 22 ps becomes less pronounced. Based on this feature, we can attribute the long time constant of 125 ps to the photocarrier lifetime in $MoSe_2$. The fast decay channel at higher fluence can be attributed to the contribution of exciton–exciton annihilation.[50]

Figure 2(b) summarizes the peak differential reflectivity signal as a function of the pump fluence. A linear relation is clearly observed, as confirmed by the linear fit (red line). Finally, with a fixed pump fluence of 1.23 μJ/cm^2, we repeated the measurement with different probe photon energies. Figure 2(c) shows the peak differential reflectivity signal as a function of the probe photon energy. The peak signal was observed at a probe photon energy of 1.57 eV, which is well consistent with the previously determined optical bandgap of $MoSe_2$ monolayers. This observation shows that the probe pulse senses the photocarriers via the change of the excitonic absorption peak induced by these carriers.

Figure 3 shows the results of the same measurement performed with the graphene–$MoSe_2$ heterostructure. If there was no interlayer photocarrier transfer or no interlayer coupling, the results should have been similar to those shown in Fig. 2. Due to the smaller absorption coefficient of graphene compared to $MoSe_2$, the carriers injected in graphene can be neglected for simplicity, and the pump pulse can be assumed to inject the same carrier density in the $MoSe_2$ of the heterostructure as the $MoSe_2$ monolayer. However, we observed two dramatic differences between the two measurements. First, the signal magnitude is about a factor of 10 larger in the heterostructure sample under the same conditions. Second, the signal decays rapidly compared to the $MoSe_2$ monolayer. Exponential fits (blue curves) produced a decay time constant of 8.5 ps. Meanwhile, similar dependences on the pump fluence and probe photon energy are observed.

We attribute these observed features to two physical mechanisms. First, the photocarriers excited in $MoSe_2$ rapidly transfer to graphene. Second, the carriers in graphene can induce a differential reflectivity signal of the probe tuned to the $MoSe_2$ resonance.

The strong dependence of the peak signal on probe photon energy indicates that the signal originates from a change of the absorption coefficient of $MoSe_2$. However, this change cannot be induced by the photocarriers in $MoSe_2$, since in the

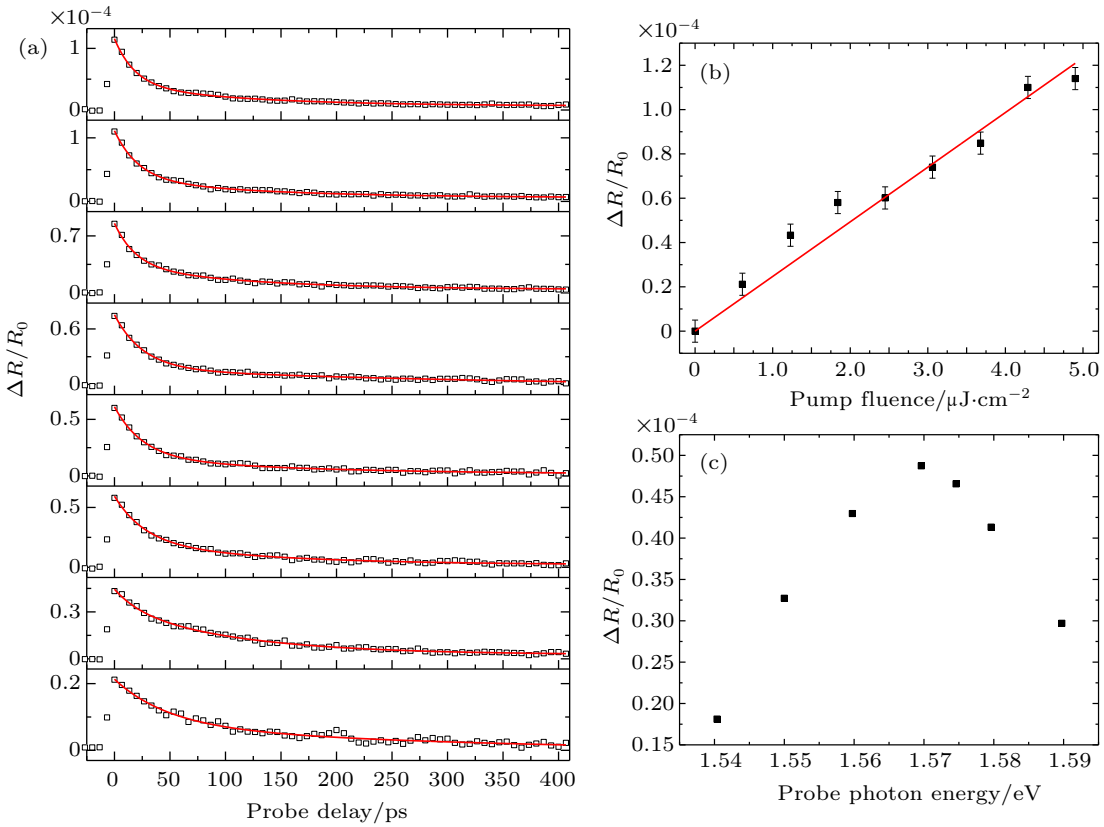


Fig. 2. (color online) Differential reflectivity measurement of monolayer $MoSe_2$. (a) Differential reflectivity signal as a function of probe delay with pump fluences of (from top to bottom) 4.9, 4.29, 3.06, 2.45, 1.84, 1.23 and 0.61 μJ/cm^2, respectively. The red curves are exponential fits. (b) Peak differential reflectivity signal as a function of pump fluence. (c) Peak differential reflectivity signal as a function of the probe photon energy.

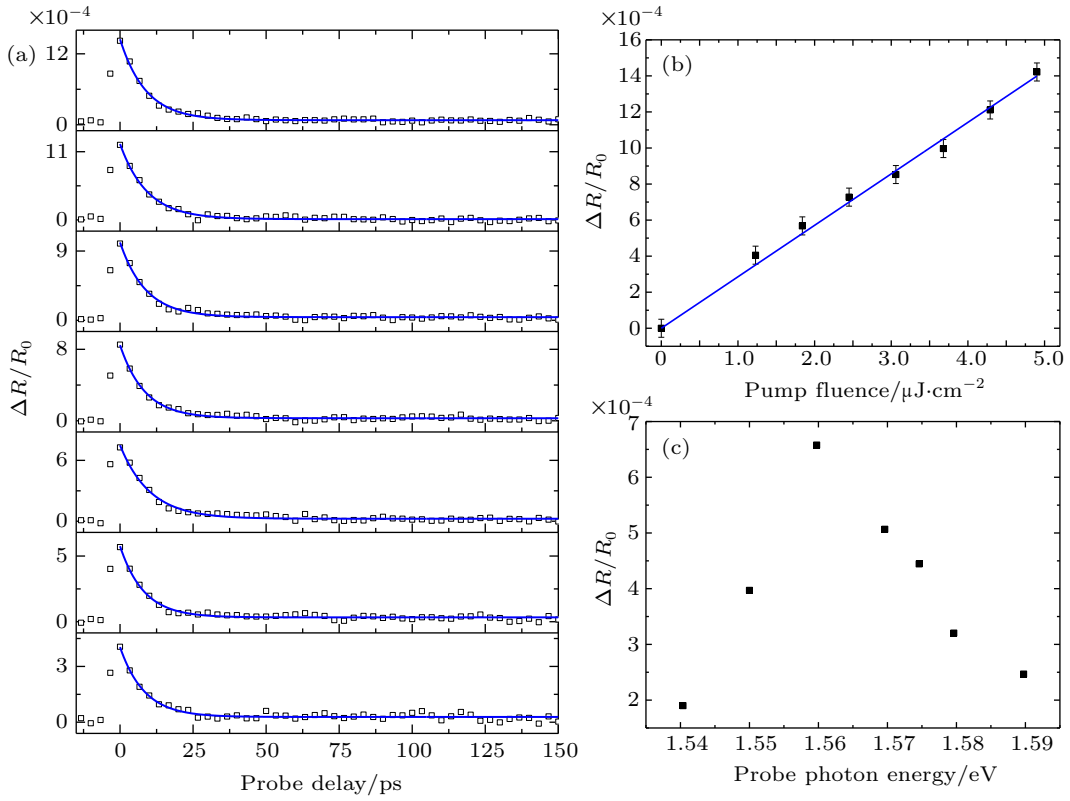


Fig. 3. (color online) Differential reflectivity measurement of graphene–$MoSe_2$ heterostructure. (a) Differential reflectivity signal as a function of probe delay with pump fluences of (from top to bottom) 4.9, 4.29, 3.06, 2.45, 1.84 and 1.23 μJ/cm^2, respectively. The blue curves are exponential fits. (b) Peak differential reflectivity signal as a function of pump fluence. (c) Peak differential reflectivity signal as a function of the probe photon energy.

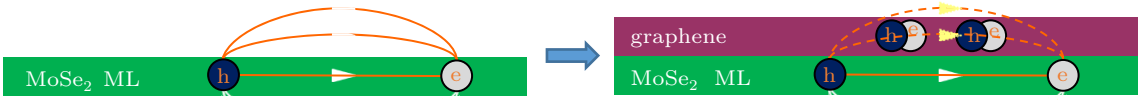


Fig. 4. The electric field of the excitons in $MoSe_2$ before and after forming the heterostruture.

measurements on $MoSe_2$ monolayer (Fig. 2), we have established the magnitude of the signal for such photocarrier densities used in the measurements. The signal is too large to be attributed to photocarriers in $MoSe_2$. Furthermore, the decay of the signal is very fast. Since the lifetime of photocarriers in graphene was known to be on the same time scale, this further indicates that the signal monitors the carriers in graphene, instead of $MoSe_2$.

We assume that the mechanism for change of the absorption coefficient of $MoSe_2$ by carriers in graphene is via a screening effect of these carriers on the electric field of the excitons. It has been well established that the Coulomb interaction between electrons and holes in monolayer TMDs is significantly enhanced by the reduced dielectric screening. As shown in Fig. 4, the majority of the field lines are in the vacuum surrounding the monolayer. This effect has resulted in extremely large exciton binding energies in these materials. When combined with a graphene layer, the carriers in graphene can screen the fields in that layer, and hence change the interaction between the electrons and holes in excitons.

Therefore, our results provide quantitative information on the physics mechanism of screening of graphene on many-body interactions in $MoSe_2$ monolayers. In particular, it is possible to control the electron–hole interaction in $MoSe_2$, as well as other 2D materials, by interfacing with graphene with a certain thickness. This opens up the opportunities of controlling electron–hole interactions in van der Waals materials.

Based on this mechanism and the fast decay of the signal observed in Fig. 3, as well as the lack of a long-lived signal, we conclude that photocarriers excited in $MoSe_2$ rapidly transfer to graphene. These carriers in graphene can alter the absorption of $MoSe_2$.

The observed effects have important implications on using these materials in optoelectronic devices. For example, the efficient transfer of photocarriers from $MoSe_2$ to graphene suggests that such bilayers can be used in photodetectors and

solar cells. $MoSe_2$ has a large absorption coefficient at optimal wavelength for solar cells, while graphene possesses superior charge transport performance. The bilayer structure effectively combines these advantages. The demonstrated control of $MoSe_2$ absorption by carriers in graphene can be utilized in light modulation applications where gate controlled carriers in graphene can be used to modulate absorption of light by $MoSe_2$.

4. Conclusion

We have fabricated a less investigated graphene–$MoSe_2$ heterostructure, and studied its photocarrier dynamics. We found that photocarriers injected in $MoSe_2$ transfer to graphene on an ultrafast time scale. We also found that a carrier in graphene can change the excitonic absorption of $MoSe_2$, which can be potentially used for electric control of optical absorption of $MoSe_2$. Our results illustrate that graphene–$MoSe_2$ heterostructures can effectively combine the novel optical absorption property of $MoSe_2$ and charge the transport property of graphene, for potential applications in optoelectronic devices.

References

[1] Novoselov K S, Geim A K, Morozov S V, Jiang D, Zhang Y, Dubonos S V, Grigorieva I V and Firsov A A 2004 *Science* **306** 666

[2] Novoselov K S, Geim A K, Morozov S V, Jiang D, Katsnelson M I, Grigorieva I V, Dubonos S V and Firsov A A 2005 *Nature* **438** 197

[3] Lee C, Wei X, Kysar J W and Hone J 2008 *Science* **321** 385

[4] Balandin A A, Ghosh S, Bao W, Calizo I, Teweldebrhan D, Miao F and Lau C N 2008 *Nano Lett.* **8** 902

[5] Jin Q, Dong H M, Han K and Wang X F 2015 *Acta Phys. Sin.* **64** 237801 (in Chinese)

[6] Stoller M D, Park S, Zhu Y, An J and Ruoff R S 2008 *Nano Lett.* **8** 3498

[7] Pan D, Wang S, Zhao B, Wu M, Zhang H, Wang Y and Jiao Z 2009 *Chem. Mater.* **21** 3136

[8] Becerril H A, Mao J, Liu Z, Stoltenberg R M, Bao Z and Chen Y 2008 *ACS Nano* **2** 463

[9] Chen H, Müller M B, Gilmore K J, Wallace G G and Li D 2008 *Adv. Mater.* **20** 3557

[10] Wang X, Zhi L and Müllen K 2008 *Nano Lett.* **8** 323

[11] Liu Z, Liu Q, Huang Y, Ma Y, Yin S, Zhang X, Sun W and Chen Y 2008 *Adv. Mater.* **20** 3924

[12] Liang Z J, Liu H X, Niu Y X and Yin Y H 2016 *Acta Phys. Sin.* **65** 138501 (in Chinese)

[13] Geim A K and Novoselov K S 2007 *Nat.Mater.* **6** 183

[14] Geim A K 2009 *Science* **324** 1530

[15] Liu H L, Shen C C, Su S H, Hsu C L, Li M Y and Li L J 2014 *Appl. Phys. Lett.* **105** 201905

[16] He K, Kumar N, Zhao L, Wang Z, Mak K F, Zhao H and Shan J 2014 *Phys. Rev. Lett.* **113** 026803

[17] Zeng F, Zhang W B and Tang B Y 2015 *Chin. Phys. B* **24** 097103

[18] Britnell L, Gorbachev R, Jalil R, Belle B, Schedin F, Mishchenko A, Georgiou T, Katsnelson M, Eaves L and Morozov S 2012 *Science* **335** 947

[19] Jiang J W and Park H S 2014 *Appl. Phys. Lett.* **105** 033108

[20] Elder R M, Neupane M R and Chantawansri T L 2015 *Appl. Phys. Lett.* **107** 073101

[21] Ebnonnasir A, Narayanan B, Kodambaka S and Ciobanu C V 2014 *Appl. Phys. Lett.* **105** 031603

[22] Coy Diaz H, Avila J, Chen C, Addou R, Asensio M C and Batzill M 2015 *Nano Lett.* **15** 1135

[23] Jin W, Yeh P C, Zaki N, Chenet D, Arefe G, Hao Y, Sala A, Mentes T O, Dadap J I and Locatelli A 2015 *Phys. Rev. B* **92** 201409

[24] Pierucci D, Henck H, Avila J, Balan A, Naylor C H, Patriarche G, Dappe Y J, Silly M G, Sirotti F and Johnson A C 2016 *Nano Lett.* **16** 4054

[25] Ulstrup S, Čabo A G, Miwa J A, Riley J M, Grønborg S S, Johannsen J C, Cacho C, Alexander O, Chapman R T and Springate E 2016 *ACS Nano* **10** 6315

[26] Wei Y, Ma XG, Zhu L, He H and Huang CY 2017 *Acta Phys. Sin.* **66** 087101 (in Chinese)

[27] Yu W J, Li Z, Zhou H, Chen Y, Wang Y, Huang Y and Duan X 2013 *Nat.Mater.* **12** 246

[28] Moriya R, Yamaguchi T, Inoue Y, Morikawa S, Sata Y, Masubuchi S and Machida T 2014 *Appl. Phys. Lett.* **105** 083119

[29] Yamaguchi T, Moriya R, Inoue Y, Morikawa S, Masubuchi S, Watanabe K, Taniguchi T and Machida T 2014 *Appl. Phys. Lett.* **105** 223109

[30] Zhang W, Chuu C P, Huang J K, Chen C H, Tsai M L, Chang Y H, Liang C T, Chen Y Z, Chueh Y L and He J H 2014 *Sci. Rep.* **4** 3826

[31] Moriya R, Yamaguchi T, Inoue Y, Sata Y, Morikawa S, Masubuchi S and Machida T 2015 *Appl. Phys. Lett.* **106** 223103

[32] Sata Y, Moriya R, Morikawa S, Yabuki N, Masubuchi S and Machida T 2015 *Appl. Phys. Lett.* **107** 023109

[33] Joiner C A, Campbell P M, Tarasov A A, Beatty B R, Perini C J, Tsai M Y, Ready W J and Vogel E M 2016 *ACS Appl. Mater. Inter.* **8** 8702

[34] Wang Z, Ki D K, Chen H, Berger H, MacDonald A H and Morpurgo A F 2015 *Nat. Commun.* **6** 9339

[35] Georgiou T, Jalil R, Belle B D, Britnell L, Gorbachev R V, Morozov S V, Kim YJ, Gholinia A, Haigh S J and Makarovsky O 2013 *Nat. Nanotechnol.* **8** 100

[36] Shanmugam M, Jacobs-Gedrim R, Song E S and Yu B 2014 *Nanoscale* **6** 12682

[37] Withers F, Del Pozo-Zamudio O, Mishchenko A, Rooney A, Gholinia A, Watanabe K, Taniguchi T, Haigh S, Geim A and Tartakovskii A 2015 *Nat. Mater.* **14** 301

[38] Tan H, Fan Y, Zhou Y, Chen Q, Xu W and Warner J H 2016 *ACS Nano* **10** 7866

[39] Kim K, Larentis S, Fallahazad B, Lee K, Xue J, Dillen D C, Corbet C M and Tutuc E 2015 *ACS Nano* **9** 4527

[40] Li Y, Qin J K, Xu C Y, Cao J, Sun Z Y, Ma L P, Hu PA, Ren W C and Zhen L 2016 *Adv. Funct. Mater.* **26** 4319

[41] Vishwanath S, Liu X, Rouvimov S, Mende P C, Azcatl A, McDonnell S, Wallace R M, Feenstra R M, Furdyna J K and Jena D 2015 *2D Mater.* **2** 024007

[42] Shim G W, Yoo K, Seo S B, Shin J, Jung D Y, Kang I S, Ahn C W, Cho B J and Choi S Y 2014 *ACS Nano* **8** 6655

[43] Ji J T, Zhang A M, Xia T L, Gao P, Jie Y H, Zhang Q and Zhang Q M 2016 *Chin. Phys. B* **25** 077802

[44] Shin B, Zhu Y, Bojarczuk N A, Chey S J and Guha S 2012 *Appl. Phys. Lett.* **101** 053903

[45] Shin B, Bojarczuk N A and Guha S 2013 *Appl. Phys. Lett.* **102** 091907

[46] Shi Y, Hua C, Li B, Fang X, Yao C, Zhang Y, Hu Y S, Wang Z, Chen L and Zhao D 2013 *Adv. Funct. Mater.* **23** 1832

[47] Guo Y and Robertson J 2016 *Appl. Phys. Lett.* **108** 233104

[48] Yu YJ, Zhao Y, Ryu S, Brus L E, Kim K S and Kim P 2009 *Nano Lett.* **9** 3430

[49] Beal A R and Hughes H P 1979 *J. Phys. C: Solid State Phys.* **12** 881

[50] Kumar N, Cui Q, Ceballos F, He D, Wang Y and Zhao H 2014 *Phys. Rev. B* **89** 125427